Thermal Removal of Mercury in Spent Powdered Activated Carbon from TOXECON Process

George D. O. Okwadha[1]; Jin Li, Ph.D.[2]; Bruce Ramme, Ph.D., P.E., M.ASCE[3]; Dave Kollakowsky[4]; and Dave Michaud[5]

Abstract: This research developed and demonstrated a technology to liberate Hg adsorbed onto powdered activated carbon (PAC) by the TOXECON process using pilot-scale high temperature air slide (HTAS) and bench-scale thermogravimetric analyzer (TGA). The HTAS removed 65, 83, and 92% of Hg captured with PAC when ran at 900°F, 1,000°F, and 1,200°F, respectively, while the TGA removed 46 and 100% of Hg at 800°F and 900°F, respectively. However, addition of $CuO-Fe_2O_3$ mixture and CuCl catalysts enhanced Hg removal and PAC regeneration at lower temperatures. $CuO-Fe_2O_3$ mixture performed better than CuCl in PAC regeneration. Scanning electron microscopy images and energy dispersive X-ray analysis show no change in PAC particle aggregation or chemical composition. Thermally treated sorbents had higher surface area and pore volume than the untreated samples indicating regeneration. The optimum temperature for PAC regeneration in the HTAS was 1,000°F. At this temperature, the regenerated sorbent had sufficient adsorption capacity similar to its virgin counterpart at 33.9% loss on ignition. Consequently, the regenerated PAC may be recycled back into the system by blending it with virgin PAC.

DOI: 10.1061/(ASCE)EE.1943-7870.0000074

CE Database subject headings: Activated carbon; Mercury; Metals, chemical; Adsorption; Abatement and removal; Thermal factors.

Introduction

Mercury, a naturally occurring element, is released into the environment by both natural sources, e.g., volcanic activity, weathering of the earth's crust, bioactivity, and anthropogenic activities. According to the EPA's 1997 mercury study report to congress, coal-fired electric utilities, municipal waste combustors, and medical waste incinerators emit the highest amounts of Hg into the air (EPA 1997). On March 15, 2005, the EPA issued the clean air mercury rule (CAMR), the first ever federal rule aimed at permanently reducing mercury emissions from coal-fired power plants. When fully implemented, CAMR would have reduced utility Hg emissions from 48 to 15 t/year by 2018, a nearly 70% reduction (EPA 2005). On February 8, 2008, the D.C. Court of Appeals vacated the CAMR. As of this time, there is no federal mercury control regulation for utility boilers. However, numerous states have enacted mercury control regulations for utility boilers, which are as or more stringent than CAMR. These mandatory caps, coupled with significant penalties for noncompliance, will ensure that mercury reduction requirements in these states are achieved and sustained (EPA 2005). In anticipation of CAMR, scientists and organizations in collaboration with the EPA and the DOE are conducting research to understand the science of mercury speciation and the fate and transport of various forms of Hg within the atmosphere to develop more efficient and cost-effective Hg control technologies and devices. In one important and unique study, the TOXECON process, which integrates Hg and particulate matter emission control systems, is being evaluated at the We Energies' Presque Isle Power Plant (PIPP) and cofunded by We Energies and DOE's Clean Coal Power Initiative.

The use of activated carbon as a sorbent to remove elemental mercury from coal combustion flue gas is widely accepted as one of the most developed and commercially viable alternative. In this case, activated carbon is injected into the flue gas downstream of a primary particulate collection device and upstream of a second particulate collection device, commonly referred to as TOXECON technology. The activated carbon and mercury mixture is collected separately from the fly ash, thereby preserving the quality of fly ash for use in concrete production. Results from previous bench-scale study (Li et al. 2005) indicate that there is a potential to liberate elemental mercury and regenerate and reuse exhausted activated carbon through thermal desorption, which would significantly reduce the cost associated with the TOXECON process.

Activated carbon is an amorphous carbon in which a high degree of porosity has been developed during manufacture. This porosity together with high surface area determine the performance of its intended function—adsorption. In general, activated carbon is sometimes described as having a "crumpled" layered surface, in which flat sheets are broken and curved back upon themselves (Efremenko and Sheintuch 2006). This unique struc-

[1]Ph.D. Student, Dept. of Civil Eng. and Mechanics, Univ. of Wisconsin-Milwaukee, Milwaukee, WI 53201. E-mail: gokwadha@uwm.edu

[2]Associate Professor, Dept. of Civil Eng. and Mechanics, Univ. of Wisconsin-Milwaukee, Milwaukee, WI 53201 (corresponding author). E-mail: li@uwm.edu

[3]Manager, Land Quality, We Energies, 333 W. Everett St., Milwaukee, WI 53203. E-mail: bruce.ramme@we-energies.com

[4]Senior Environmental Consultant, We Energies, 333 W. Everett St., Milwaukee, WI 53203. E-mail: dave.kollakowsky@we-energies.com

[5]Principal Environmental Consultant, We Energies, 333 W. Everett St., Milwaukee, WI 53203, dave.michaud@we-energies.com

Note. This manuscript was submitted on October 22, 2008; approved on February 23, 2009; published online on February 26, 2009. Discussion period open until March 1, 2010; separate discussions must be submitted for individual papers. This paper is part of the ***Journal of Environmental Engineering***, Vol. 135, No. 10, October 1, 2009. ©ASCE, ISSN 0733-9372/2009/10-1032–1040/$25.00.

ture creates activated carbon's very large surface area (Pope 1996). The large surface area provides many sites (CPL Carbon Link 2006) upon which the adsorption of impurity molecules takes place (Martin and Ng 1987; Skodras et al. 2005; Henning and Schafer 1990). In these sites, pores of different sizes with specific functions exist. The distribution of these pores is the principal factor determining the adsorption characteristics of activated carbon (Chiang et al. 2001; San Miguel et al. 2001). Once the surface area is covered by the adsorbates, adsorption ceases and breakthrough occurs. The spent adsorbent must therefore be processed to remove the adsorbate before the carbon can be used again. Processing involves regeneration of the carbon to restore the pore structure, volume, and distribution. According to Sing et al. (1985) and Bansal et al. (1988), pores are classified into three categories based on their sizes. *Macropores* are cavities of diameter greater than 50 nm, used as entrance to the activated carbon by adsorbate molecules. *Mesopores* are pores of diameter between 2 and 50 nm and are used for transportation and adsorption of larger molecules, which cannot gain access to smaller pores. *Micropores* are the smallest category of pores. Their diameter is less than 2 nm and provides activated carbon with most of their surface area and adsorption characteristics (Henning and Schafer 1990).

Adsorption capacity of activated carbon depends on surface area of the activated carbon, adsorption temperature, porosity, pore-size distribution, concentration of the adsorbates, type of adsorbate, and the oxygen functional groups in the active centers of the activated carbon (Efremenko and Sheintuch 2006; Skodras et al. 2005; San Miguel et al. 2001; Li et al. 2002, 2003; Ania et al. 2005; Brennan et al. 2002). Mercury adsorption, in particular, is influenced by many factors including the type of mercury being adsorbed, flue gas composition, adsorption temperature, the inlet mercury concentration, and the gas flow rate (Carey et al. 1998; Ho et al. 2004). Efremenko and Sheintuch (2006), Mundale et al. (1991), and Demirbas et al. (2006) have indicated that the high adsorption capacity of activated carbon is attributed to the surface oxygen functional groups. Studies done by Skodras et al. (2005) and Li et al. (2002, 3) have shown that lactone and carbonyl functional groups are the active sites for elemental mercury (Hg^0) adsorption. However, these oxygen complexes may be removed from activated carbon surface by heating to 990°C (Mundale et al. 1991; Walker et al. 1991) or repeated reuse and regeneration. This is one of the reasons why activated carbon lose adsorption capacity overtime upon regeneration (Mundale et al. 1991).

The objective of the present study was to evaluate the possibility of liberating Hg adsorbed on the PAC captured by the TOXECON process by thermal methods at the bench scale using a thermogravimetric analyzer (TGA) and at the pilot scale using a high temperature air slide apparatus (HTAS), with and without the addition of transition metal oxide catalysts. The efficiency of Hg removal from the PAC was determined by measuring the total Hg that was left in the sample after thermal treatments. The regenerated carbon samples were evaluated in terms of changes in the external pore structure by a scanning electron microscopy (SEM), the Brunauer, Emmett, and Teller (BET) surface area and the Barrett, Joyner, and Halenda (BJH) average pore-size and pore-volume distribution tests. The remaining adsorptive capacity was determined by testing packed beds containing spent PAC in a slip stream of flue gas produced at PIPP. The chemical composition of regenerated PAC (RPAC) was determined by energy dispersive X-ray (EDX) while carbon losses by thermal desorption testing was measured by loss on ignition (LOI) test.

Experimental Methods

Materials

The lignite-based PAC containing Hg captured by the TOXECON process was obtained from the PIPP facility in Marquette, Michigan and the samples were used as delivered. Brominated (Darco Hg-LH) and nonbrominated (Darco Hg) PAC were used. A mixture of 1% copper (II) oxide, (CuO) powder and 4% iron (III) oxide, (Fe_2O_3) powder, and cuprous chloride (CuCl) powder (Sigma-Aldrich Corp., Wisconsin) with purity of 99.99, 99, and 97%, respectively, were used as catalysts in the experiment. The iron (III) oxide powder had a nominal size of 5 μm (manufacturer's specification), whereas copper (I) chloride powder and copper (II) oxide powder were of reagent grade. The copper-iron oxides were mixed by agitation using a mechanical tumbler and was selected following a successful use by Matatov-Meytal and Sheintuch (1997), Sheintuch and Matatov-Meytal (1999), and Matatov-Meytal et al. (1997), whereas CuCl had been successfully used by Ghorishi et al. (2005).

Bench-Scale Study in the Thermogravimetric Analyzer

Hg was liberated and exhausted PAC was regenerated in a TGA-500 (Leco Corporation, Mich.) device at the bench scale. The thermal stability of the PAC samples was measured by comparing the weight loss exhibited by the samples following heat treatment. The TGA was run in an inert atmosphere with a N_2 flow rate of 100 mL/min to prevent ignition of the PAC during heating. The heating rate was 10°C/min until the target temperature was reached. The target temperature was maintained for 2 h before the sample was allowed to cool at room temperature in an inert (N_2) atmosphere. The crucibles were covered to help maintain the inert atmosphere. The working temperatures were chosen based on research results reported by Avraamides (1987), Van Vliet (1991), Ferro-Garcia et al. (1993), Matatov-Meytal and Sheintuch (1997), Sheintuch and Matatov-Meytal (1999), Matatov-Meytal et al. (1997), Bagreev et al. (2002), Manocha (2003), and Li et al. (2002, 3).

Pilot-Scale Study in the High Temperature Air Slide

Based upon the test results obtained from the bench-scale study, a test program was designed to generate experimental data from a pilot-scale HTAS apparatus (Fig. 1). The detailed configuration of the apparatus was previously described by Li et al. (2005). Briefly, the whole system is divided into five components: a conical hopper, an air slide, a baghouse, a burner, and a collector at the end of the air slide. During each experiment, the samples were fed into the air slide through the conical hopper. A rotary feeder controlled the speed at which the sample entered the treatment system. Inside the air slide, the samples were heated by the hot air generated by the gas fuel burner. The temperature inside the air slide was controlled by adjusting the air flow rate to the gas burner. After the thermal treatment, the product sample went to the collector underneath the air slide and the processed by-products (mostly mercury, particulate, and volatile materials driven off the PAC samples) went to the baghouse.

BET Surface Area and BJH Pore-Size Distribution

The BET surface area and BJH pore-size volume analyses were done in accordance with ASTM D3663 (ASTM 2008) and ASTM

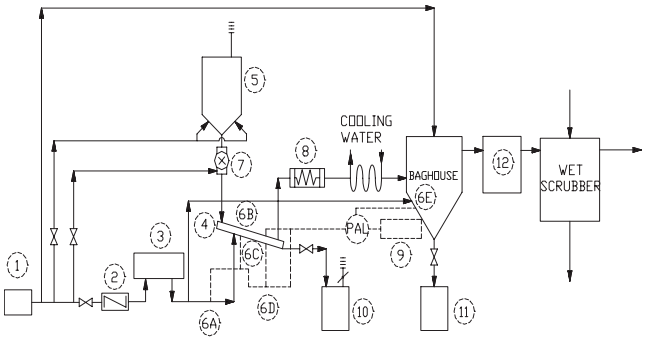

Fig. 1. Schematic diagram of the pilot-scale HTAS apparatus for mercury liberation and capture: (1) air supply; (2) heat exchanger; (3) 1,500°C furnace; (4) air slide; (5) spent PAC sample feeder; (6A)-(6E), thermo couples; (7) rotary feeder; (8) heat exchanger; (9) control panel; (10) product collection drum; (11) by-product collection drum; and (12) mercury condenser (Li et al. 2005)

D4641-94 (ASTM 2006), respectively, using a Micromeritics VacPrep 061 sample degas system (Micromeritics, Norcross, Georgia) and a Micromeritics TriStar 3000 surface area and porosity analyzer (Micromeritics, Norcross, Ga.). Representative samples of 0.2 g were degassed under vacuum of 27 mTorr (0.04 mBar) at 100°C for 24 h to remove moisture and other contaminants. High purity nitrogen was used as the adsorptive gas for analysis and liquid nitrogen (maintained at −195.8°C) as the cryogen for maintaining a constant bath temperature. Surface area, pore size, and pore volume distribution were determined using BET and BJH theories, respectively.

Adsorption Capacity of the Regenerated Power Activated Carbon Sorbent

The adsorption capacity of the RPAC sorbent was evaluated using a slip-stream reactor at Presque Isle Power plant (PIPP) in Marquette, Mich. The plant's mercury continuous emission monitor was used to measure the outlet total mercury levels. Two virgin PAC (VPAC) sorbents, Darco Hg (nonbrominated) and Darco Hg-LH (brominated), were prepared by adulterating them with PIPP fly ash to 33.9 and 44.1% LOI, respectively, to mimic the spent PAC sample used before the thermal treatment for the purpose of determining whether full regeneration of the spent PAC sample occurred.

Sample Analysis

The total Hg was determined using the cold-vapor atomic absorption method, commonly referred to as the EPA method 7471A/245.7 with a precision of ±15% and a minimum detection limit of 0.012 ppm. Moisture content and LOI were determined in accordance with ASTM methods D5142 and C311, respectively. A SEM (ABT-32, Topcon America Corporation, New Jersey) coupled with EDX microanalysis were used to obtain representative images and chemical composition of the PAC samples before and after the thermal treatments.

Results and Discussion

Bench-Scale Feasibility Study Using the Thermogravimetric Analyzer

Table 1 shows sample descriptions. The bench-scale tests were performed in the TGA in an inert atmosphere for 2 h. As shown in Table 2, Hg removal was 46% at 800°F and 100% at temperatures of 900°F and higher in the absence of a catalyst. With the addition of catalysts, i.e., a mixture of 1% CuO and 4% Fe_2O_3 and 5% CuCl, complete removal of Hg from the PAC occurred at a lower temperature (700°F). These results are in agreement with previous studies which reported that higher Hg removal can be achieved at lower temperatures with catalysts (Matatov-Meytal et al. 1997; Sheintuch and Matatov-Meytal 1999; Dranca et al. 2001; Manocha 2003; Ramme et al. 2007; Coss and Chang 2000).

LOI is used as an indicator of carbon content in the PAC since, in this case, carbon is the main component of the sorbent. Fig. 2 presents the influence of temperature on processed sample LOI with and without catalysts after thermal treatment in the TGA. The results show that the processed sample's LOI decreased when the treatment temperature increased, which indicates possible carbon loss in the PAC during the treatment process. There is a sharp decrease in the LOI for catalyst-treated PAC compared with the PAC thermally treated without catalysts.

Table 3 shows BJH average pore diameter, BJH cumulative volume and surface area of pores between 17 and 3,000-Å diameter, and BET surface area test results. The pore size range between 17 and 3,000-Å diameter were chosen because it covers the pore size range of this PAC from micropores to macropores and is also the limit of the nitrogen adsorption and desorption technique. Thermal treatment at 700°F without addition of catalysts increased the surface area and cumulative surface area of pores between 17 and 3,000-Å diameter by 27 and 19%, respectively. At this temperature, pore volume increased by 15%, whereas average pore diameter decreased by an average of 2%. This result indicates that 700°F is the optimum temperature for regenerating this type of PAC because thermal treatment beyond this temperature gave lower adsorption parameters. Addition of CuO and Fe_2O_3 mixture also increased the surface area but by only 14%. However, the CuCl catalyst did not improve adsorption parameters of this brominated PAC. It is believed that bromine in the PAC might have suppressed the activity of this catalyst. Cao et al. (2007) reported that at higher temperatures (in the range of 300–350°C), simultaneous formation of $HgBr_2$ and $HgCl_2$ occur in the flue gas. Bromine attacks chlorine species to generate activated chlorine. SO_2 in the flue gas then consumes all the activated chlorine, reducing in concentration and, in the process, enhances Hg oxidation (Cao et al. 2007). This explanation suggests that, depending on the concentration of Cl_2 in the flue gas, it is possible that CuCl might become a rich source of Cl_2 for this purpose. This could reduce the catalytic role of CuCl.

Pilot-Scale Study

As shown in Table 4, the Hg removal rates from the thermally treated PAC samples were 65, 83, and 92% at 900, 1,000, and 1,200°F, respectively, in the HTAS. It is noted that although 100% Hg removal was achieved in the TGA bench-scale test at 800°F, the PAC retention time in the air slide was only a few seconds as compared with the 2 h retention time in the TGA. Consequently, we cannot compare Hg removal efficiency by the HTAS with the TGA but treat each individual device indepen-

Table 1. Sample Description, Type of PAC, and Condition

Sample number	Sample description	Type of PAC
A1	Product sample after thermal treatment at 1,000°F for a few seconds in the HTAS	Darco Hg with fly ash at LOI 33.9%
A2	Product sample after thermal treatment at 1,200°F for a few seconds in the HTAS	Darco Hg-LH with fly ash at LOI 44.1%
A3	By-product (baghouse) sample after thermal treatment at 1,000°F for a few seconds in the HTAS	Darco Hg with fly ash at LOI 33.9%
A4	By-product (baghouse) sample after thermal treatment at 1,200°F for a few seconds in the HTAS	Darco Hg-LH with fly ash at LOI 44.1%
B1	Untreated (as delivered) sample	Darco Hg with fly ash at LOI 33.9%
T1	Product sample after thermal treatment at 700°F for 2 h in an inert atmosphere in the TGA	Darco Hg-LH with fly ash at LOI 44.1%
T2	Product sample after thermal treatment at 800°F for 2 h in an inert atmosphere in the TGA	Darco Hg-LH with fly ash at LOI 44.1%
T3	Product sample after thermal treatment at 1,000°F for 2 h in an inert atmosphere in the TGA	Darco Hg-LH with fly ash at LOI 44.1%
T4	Product sample after thermal treatment at 1,100°F for 2 h in an inert atmosphere in the TGA	Darco Hg-LH with fly ash at LOI 44.1%
T5	Product sample with a mixture of 1% CuO and 4% Fe_2O_3 catalyst after thermal treatment at 700°F for 2 h in an inert atmosphere in the TGA	Darco Hg-LH with fly ash at LOI 44.1%
T6	Product sample with a mixture of 1% CuO and 4% Fe_2O_3 catalyst after thermal treatment at 900°F for 2 h in an inert atmosphere in the TGA	Darco Hg-LH with fly ash at LOI 44.1%
T7	Product sample with a mixture of 5% CuCl catalyst after thermal treatment at 700°F for 2 h in an inert atmosphere in the TGA	Darco Hg-LH with fly ash at LOI 44.1%
T8	Product sample with a mixture of 5% CuCl catalyst after thermal treatment at 900°F for 2 h in an inert atmosphere in the TGA	Darco Hg-LH with fly ash at LOI 44.1%

dently. The product sample collected at discharge end of the air slide had a lower Hg content than the processed by-product sample collected in the baghouse. Similar observations were made by Li et al. (2005) during a pilot-scale test with the fly ash. Samples collected from the baghouse also contained moisture as compared to those collected under the air slide. The most probable cause of this phenomenon could be that the baghouse cooling water provided a cooler condensing environment for the moisture present in the PAC samples which was vaporized upon heating. There was no trend in the variation in LOI with temperature for the samples tested in the HTAS (Table 4).

The surface area and cumulative surface area of pores between 17 and 3,000-Å diameter (Table 3) of the product sample collected under the HTAS after thermal treatment at 1,000°F increased by 22 and 15%, respectively. However, raising the thermal treatment temperature to 1,200°F reduced the surface area, cumulative surface area and volume of pores between 17 and 3,000-Å diameter, and average pore diameter by 25, 28, 30, and 2%, respectively. This could be because temperatures above 1,000°F exerted high thermal stresses that volatilized the PAC and, in the process, destroyed its physical structure and the active sites on the surface that are responsible for adsorption. The other explanation could be that high temperatures might have promoted the adsorption of other substances onto the PAC surface, clogging pores, resulting in low pore volumes.

Table 2. Effect of Temperature on Mercury Removal Using the Bench-Scale TGA When a Mixture of 1% CuO and 4% Fe_2O_3 and 5% CuCl Catalysts Are Added and When No Catalyst Is Added and Run for 2 h in an Inert Atmosphere

Temperature (°F)		500	700	800	900	1,000	1,100
After the test (no catalyst)	Hg content (ppm)	—	—	29.0	0.0	0.0	0.0
	% Hg removed	—	—	46.0	100.0	100.0	100.0
	LOI	—	—	38.3	35.9	34.4	31.6
After the test with PAC +1% CuO +4% Fe_2O_3	Hg content (ppm)	58.0	1.4	—	0.0	—	—
	% Hg removed	−7.4[a]	97.4	—	100.0	—	—
	LOI	40.9	35.9	—	32.6	—	—
After the test with PAC+5% CuCl	Hg content (ppm)	64.0	0.0	—	0.0	—	—
	%Hg removed	−18.5[a]	100.0	—	100.0	—	—
	LOI	40.6	35.0	—	31.7	—	—

Note: Initial Hg Content and LOI Were 54 ppm and 44.1%, respectively.

[a]Negative values indicate that mercury content has increased probably due to contamination from the equipment.

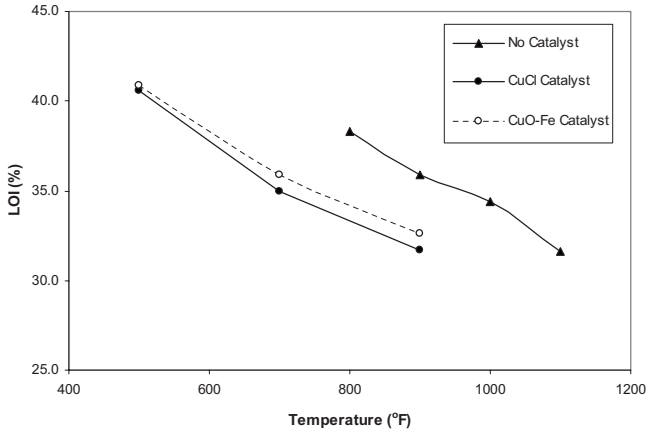

Fig. 2. Effect of temperature on LOI for spent PAC samples heated for 2 h in an inert atmosphere in the TGA with the addition of a mixture of 1% CuO and 4% Fe_2O_3 catalyst and 5% CuCl catalyst and without catalysts

SEM Analysis

The SEM images were taken at different positions of the sample to examine the morphologic changes prior to and after the thermal treatment. As shown in Fig. 3, the samples are composed of fine and coarse particles with the white round particles being mainly fly ash spheres of inorganic compounds and the relatively dark particles being mostly unburned PAC. The SEM images of the as-delivered PAC sample [Fig. 3(a)] and samples from the TGA test at 700°F without [Fig. 3(b)] and with [Fig. 3(d)] catalysts were compared. Results indicate no carbon loss and no change in particle aggregation in the sample without catalyst [Fig. 3(b)] while fine aggregation and moderate carbon loss was observed in the sample treated with Fe_2O_3–CuO mixture catalyst [Fig. 3(d)]. When the treatment temperature was increased to 900°F and catalysts were added [Fig. 3(e)], no particle aggregation and moderate carbon loss was observed with Fe_2O_3–CuO mixture catalyst. However, no particle aggregation and carbon loss was observed with CuCl catalyst [Fig. 3(f)]. The probable cause of carbon loss and particle aggregation at 700°F and beyond in the TGA with the addition of catalysts could be that the optimum temperature for catalytic oxidation might have been exceeded causing partial volatilization of the PAC.

Similarly, the SEM images from the pilot-scale HTAS tested at 1,200°F were also compared with the as-delivered PAC sample image. Fine aggregation and moderate carbon loss in the bed product image [Fig. 3(h)] was observed. However, when the TGA and HTAS samples both treated at 1,000°F [Figs. 3(c and g), respectively] were compared, the HTAS sample exhibited no change in particle aggregation but fine aggregation was observed in the TGA sample. In addition, the TGA samples exhibited moderate carbon loss, whereas the HTAS sample did not. The fine aggregation and carbon loss observed in the HTAS sample when treated at temperatures beyond 1,000°F could be attributed to partial volatilization of the PAC.

Analysis of EDX was performed on the PAC samples before and after thermal treatment to provide relative comparisons of elements in the PAC for the purpose of determining changes, if any, in the chemical composition of the particles. The analysis was done on the coarse particles within a selected representative area. Results presented in Fig. 4 show that the fine particles are composed of fly ash particles with high aluminum, silicon, and magnesium peaks [Figs. 4(a and c)], whereas the coarse particles show high carbon peaks and are composed of calcium and sulfur [Figs. 4(b and d)]. It is believed that calcium and sulfur might have been adsorbed on the carbon surface or reflected the original source of the sorbent (lignite coal). Moreover, the addition of catalysts did not affect the chemical composition of the particles. All the PAC samples showed high calcium content, which is likely attributable to the PRB coal fly ash.

Adsorption Capacity of the Regenerated PAC Sorbent

Figs. 5 and 6 show the adsorption capacity of the TGA and the HTAS regenerated samples, respectively. The results indicate that all TGA and HTAS treated samples had 26 and 15% higher adsorption capacity, respectively, than the untreated spent PAC at resident times of up to 15 min. However, beyond this time, their

Table 3. Surface Area, Pore Volume, and Pore-Size Test Results

Sample number	Surface area (m^2/g)			Pore volume (cm^3/g)		Pore size (Å)	
		BJH cumulative surface area of pores between 17 and 3,000-Å diameter		BJH cumulative volume of pores between 17 and 3,000-Å diameter		BJH average pore diameter (4 V/A)	
	BET surface area	Adsorption	Desorption	Adsorption	Desorption	Adsorption	Desorption
A1	237.96	146.95	151.36	0.22	0.22	60.21	58.76
A2	146.44	92.18	95.12	0.14	0.14	60.68	59.02
A3	205.04	130.07	133.54	0.21	0.21	65.20	63.63
A4	83.52	57.06	57.29	0.09	0.09	62.23	61.55
B1	195.18	126.32	133.50	0.20	0.20	62.16	59.36
T1	247.90	151.34	157.83	0.23	0.23	60.52	58.59
T2	217.79	137.85	142.70	0.20	0.20	57.91	56.10
T3	231.62	144.68	149.28	0.21	0.21	57.63	56.09
T4	231.01	150.70	155.34	0.23	0.23	60.13	58.57
T5	220.44	147.75	153.46	0.22	0.22	58.80	57.02
T6	221.84	141.38	147.85	0.22	0.22	60.87	58.75
T7	143.51	115.43	123.06	0.18	0.19	63.91	60.79
T8	143.07	118.29	126.95	0.19	0.20	65.66	62.14

Table 4. Effect of Temperature on Mercury Removal Using the Pilot-Scale HTAS after Being Run for a Few Seconds at a Constant Rotary Feed Speed of 1,200 rpm

Rotary feed speed (rpm)		1,200		
Temperature (°F)		900	1,000	1,200
Sample as delivered	Hg content (ppm)	37.00	37.00	46.00
	LOI	33.90	33.90	44.10
Sample collected under the air slide (product)	Hg content (ppm)	13.00	6.40	3.70
	% Hg removed	64.90	82.70	92.00
	LOI	27.00	41.20	17.80
Samples collected from the baghouse (by-product)	Hg content (ppm)	69.00	36.00	27.00
	LOI	26.60	35.40	27.00

adsorption capacity decreases by about 17%. The adulterated VPAC sorbents also exhibited similar behavior, indicating that at short residence times, the HTAS RPAC sorbents behave similarly to the adulterated sorbent. This behavior confirms that regeneration of the HTAS-processed PAC sorbents occurred. Consequently, blending the HTAS-RPAC sorbents with VPAC sorbent and injecting the blend back into the flue gas downstream of a primary particulate collection device but upstream of a sorbent injection system such as TOXECON is feasible because the sorbent residence time in flue gas is but a few seconds in real time. This may be done by either blending the VPAC with RPAC and mixing them together before injection into the flue gas or blending VPAC with RPAC at measured ratios before mixing and injecting both into the flue gas. Such a process may reduce costs associated with purchasing VPAC and disposing the spent PAC in landfills. The process would also potentially conserve natural resources and valuable landfill capacity.

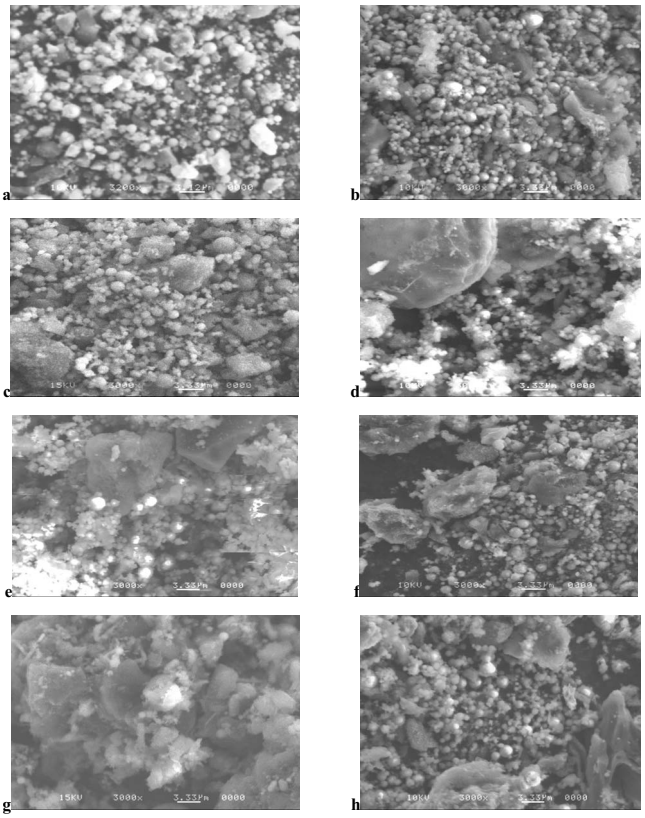

Fig. 3. SEM images of PAC samples after the TOXECON process; (a) as delivered (image is at 3200X, all others are at 3000X) ; (b) after thermal treatment in the TGA at 700°F in an inert atmosphere for 2 h without catalyst; and (c) after thermal treatment in the TGA at 1,000°F in an inert atmosphere for 2 h. After addition of a mixture of 1% CuO and 4% Fe_2O_3 catalyst and thermal treatment in the TGA in an inert atmosphere for 2 h without catalyst; (d) at 700°F; (e) at 900°F; (f) after addition of 5% CuCl catalyst and heated at 900°F in an inert atmosphere for 2 h; (g) product after thermal treatment at 1,000°F along the HTAS without addition of catalyst along the HTAS; and (h) product after thermal treatment at 1,200°F along the HTAS without addition of catalyst. [(a) image.]

Conclusions

The experimental results indicate that Hg captured with sorbent injection control equipment can be removed by both the bench-scale TGA and the pilot-scale HTAS with reasonable efficiencies. The bench-scale experiment using TGA removed 46 and 100% of Hg at operation temperatures of 800 and 900°F without catalysts while 100% Hg removal was accomplished with catalysts at temperatures as low as 700°F. The bench-scale results demonstrate that Hg can be liberated with a higher efficiency in a well controlled environment. It also demonstrates that a mixture of 1% CuO and 4% Fe_2O_3 catalyst and 5% CuCl can enhance Hg liberation at lower temperatures. The catalytic performance of 5% CuCl was identical to that of the copper oxide-iron oxide mixture. Carbon loss, as determined by LOI, was minimal but increased with temperature to a maximum of about 13% with and without catalysts.

The SEM analysis of the spent PAC samples treated in the HTAS showed no change in particle aggregation. However, particles from the TGA treated at the same 1,000°F temperature appeared finer than those from the air slide bed. This was because the TGA was more efficient in controlling heat loss and concentrated all the heat onto the samples causing their partial combustion. In general, thermal treatment at the pilot-scale HTAS had no effect on particle morphology. The EDX analysis showed that the spent PAC samples were composed of coarse and fine particles. The coarse particles were rich in calcium and sulfur embedded in a matrix of carbon and the fines were fly ash particles rich in aluminum, silicon, and magnesium. Higher BET surface area and BJH cumulative pore volume than the as-delivered sample also established that the thermal regeneration of the spent PAC samples occurred and 700 and 1,000°F are the optimum temperatures for thermal regeneration in the bench-scale TGA and pilot-scale HTAS, respectively. In addition, at this temperature the HTAS-regenerated sorbent has a higher LOI (41.2%) than its untreated counterpart (33.9%) and has also sufficient residual adsorption capacity similar to its virgin counterpart at 33.9% LOI.

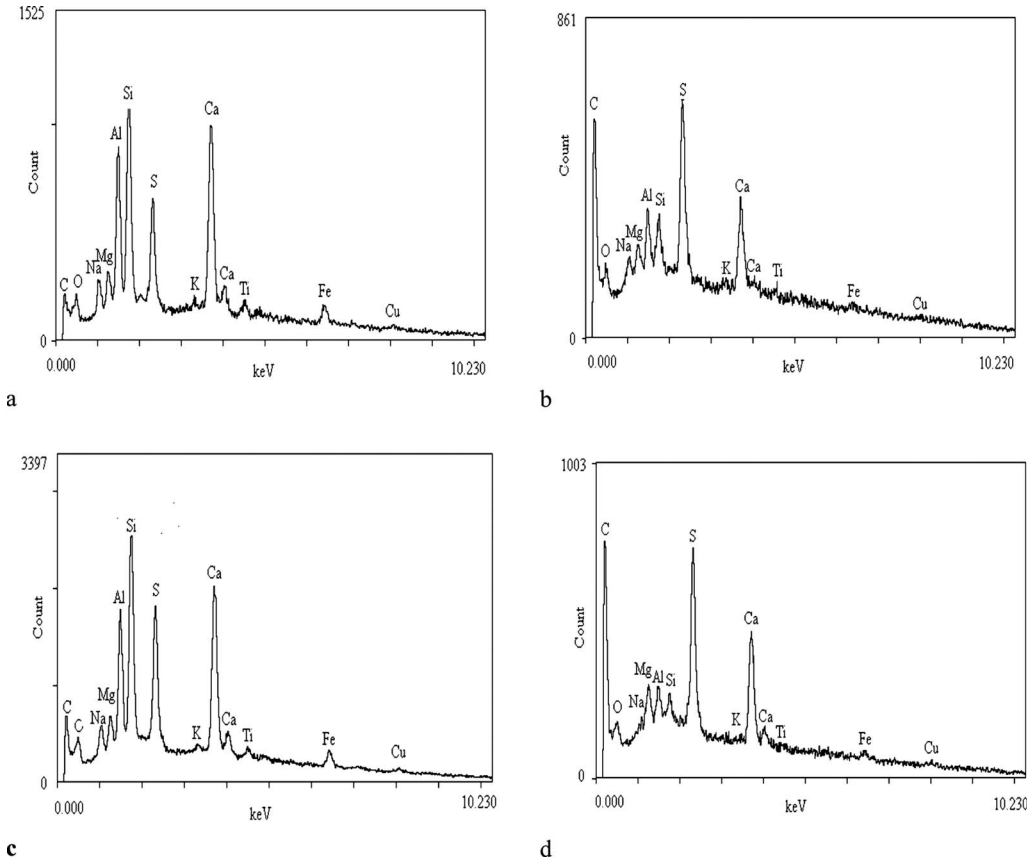

Fig. 4. (a) EDX analysis of an average PAC sample area after thermal treatment in the TGA at 1,000°F in an inert atmosphere for 2 h; (b) EDX analysis of a coarse PAC particle after thermal treatment in the TGA at 700°F for 2 h in an inert atmosphere; (c) EDX analysis of fine particles within a selected representative area of a mixture of spent PAC and 1% CuO and 4% Fe_2O_3 catalyst after thermal treatment along the HTAS (product) at 700°F; and (d) EDX analysis of a coarse spent PAC particle after addition of a mixture of 1% CuO and 4% Fe_2O_3 catalyst and heated for a few seconds along the HTAS (product) at 700°F. (All peaks are at 500X magnification.)

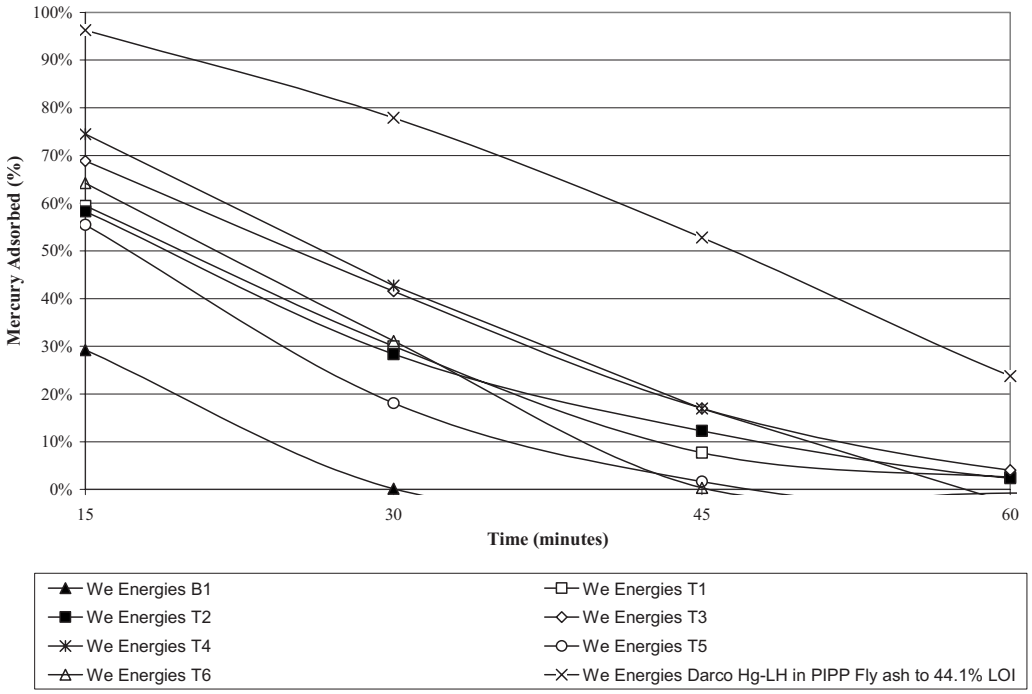

Fig. 5. Effect of time on mercury adsorption for the TGA RPAC samples. Note: for the test using Darco Hg-LH, pure Darco Hg-LH (brominated PAC) was diluted with PIPP fly ash until the LOI for the mixture was 44.1%.

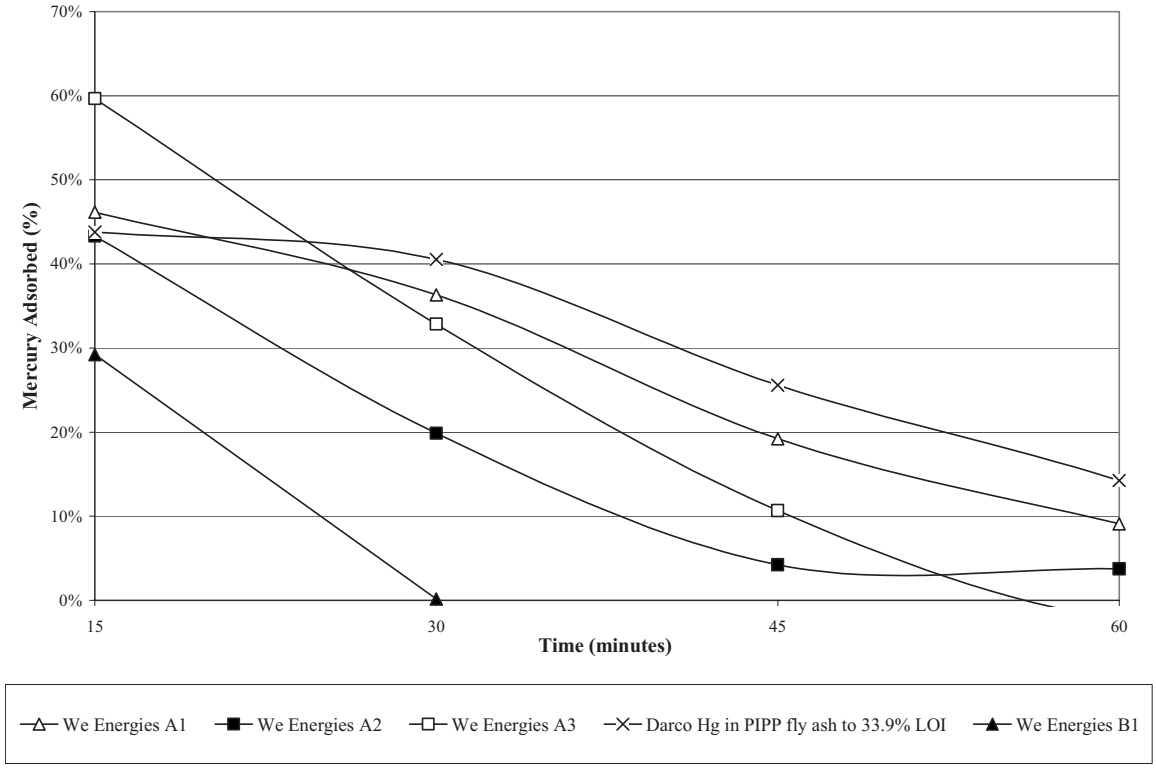

Fig. 6. Effect of time on mercury adsorption for the HTAS RPAC samples. Note: for the test using Darco Hg (nonbrominated PAC), pure Darco-Hg was diluted with PIPP fly ash until the LOI for the mixture was 33.9%.

Consequently, the RPAC may be recycled in a system by blending it with VPAC. The $CuO-Fe_2O_3$ mixture catalyst was more effective in regenerating the spent PAC than CuCl. This research also demonstrated that both thermal Hg removal and PAC regeneration can occur simultaneously.

Acknowledgments

The writers thank the University of Wisconsin System Solid Waste Research Program and We Energies for providing funds, materials, and laboratory support throughout this research project. We also thank Robin Stewart and Ken Baldrey both of ADA-ES, Inc. for the slip-stream tests involving processed PAC and VPAC at PIPP as well as for their additional laboratory testing and technical support.

References

Ania, C. O., Parra, J. B., Pevida, C., Arenillas, A., Rubiera, F., and Pis, J. J. (2005). "Pyrolysis of activated carbons exhausted with organic compounds." *J. Anal. Appl. Pyrolysis*, 74, 518–524.

ASTM. (2006). "Standard practice for calculation of pore size distributions of catalysts from nitrogen desorption isotherms." *ASTM D4641–94*, West Conshohocken, Pa.

ASTM. (2008). "Standard test method for surface area of catalysts and catalyst carriers." *ASTM D3663*, West Conshohocken, Pa.

Avraamides, J. (1987). "Thermal regeneration of activated carbons-effect of temperature, time and steam addition on carbon activity." *Trans. Inst. Min. Metall., Sect. C*, 96, 137–143.

Bagreev, A., Rahman, H., and Bandosz, T. J. (2002). "Study of regeneration of activated carbons used as H_2S adsorbents in water treatment plants." *Adv. Environ. Res.*, 6, 303–311.

Bansal, R. C., Donnet, J. B., and Stoeckli, F. (1988). *Active carbon*, Marcel Dekker, New York.

Brennan, J. K., Thomson, K. T., and Gubbins, K. E. (2002). "Adsorption of water in activated carbons: Effects of pore blocking and connectivity." *Langmuir*, 18(14), 5438–5447.

Cao, Y., et al. (2007). "Investigation of mercury transformation by HBr addition in a slipstream facility with real flue gas atmospheres of bituminous coal and powder river basin coal." *Energy Fuels*, 21, 2719–2730.

CPL Carbon Link. (2006). "Properties of activated carbon." ⟨www.activated-carbon.com/carbon.html⟩.

Carey, T. R., Hargrove, O. W., Jr., and Richardson, C. F. (1998). "Factors affecting mercury control in utility flue gas using activated carbon." *J. Air Waste Manage. Assoc.*, 48, 1166–1174.

Chiang, Y. -C., Chiang, P. -C., and Huang, C. -P. (2001). "Effects of pore structure and temperature on VOC adsorption on activated carbon." *Carbon*, 39, 523–534.

Coss, P. M., and Chang, Y. C. (2000). "Microwave regeneration of activated carbon used for removal of solvents from vented air." *J. Air Waste Manage. Assoc.*, 50, 529–535.

Demirbas, A., Arslan, G., and Pehlivan, E. (2006). "Recent studies on activated carbons and fly ashes from Turkish resources." *Energy Sources, Part A.*, 28(7), 627–638.

Dranca, I., Lupascu, T., Vogelsang, K., and Monahova, L. (2001). "Utilization of thermal analysis to establish the optimal conditions for regeneration of activated carbons." *J. Therm. Anal. Calorim.*, 64, 945–953.

Efremenko, I., and Sheintuch, M. (2006). "Predicting solute adsorption on activated carbon: Phenol." *Langmuir*, 22(8), 3614–3621.

EPA (1997). "Mercury study to congress." *Rep. No. EPA-452-R-97-003-009,* EPA, Washington, D.C.

EPA (2005). *Clean air mercury rule (CAMR)*, EPA, Washington, D.C.

Ferro-Garcia, M. A., Utrera-Hidalgo, E., Rivera-Utrilla, J., Moreno-Castilla, C., and Joly, J. P. (1993). "Regeneration of activated carbons exhausted with chlorophenols." *Carbon*, 31(6), 857–863.

Ghorishi, B. S., Lee, C. W., Jozewicz, W. S., and Kilgroe, J. D. (2005). "Effect of fly ash transition metal content and flue gas HCl/SO_2 ratio on mercury speciation in waste combustion." *Environ. Eng. Sci.*, 22(2), 221–231.

Henning, K. -D., and Schafer, S. (1990). "Impregnated activated carbon for environmental protection." *Proc., Meeting of the European Rotogravure Association Engineers Group*, Carbo Tech AC GmbH, Essen, Germany, Technical Papers #7.3, ⟨www.activated-carbon.com/carbon.htm⟩.

Ho, T. C., Kobayashi, N., Lee, Y., Lin, J., and Hopper, J. R. (2004). "Experimental and kinetic study of mercury adsorption on various activated carbons in a fixed-bed adsorber." *Environ. Eng. Sci.*, 21(1), 21–27.

Li, J., Gao, X., Goeckner, B., Kollakowsky, D., and Ramme, B. (2005). "A pilot study of mercury liberation and capture from coal-fired power plant fly ash." *J. Air Waste Manage Assoc.*, 55, 258–264.

Li, Y. H., Lee, C. W., and Gullett, B. K. (2002). "The effect of activated carbon surface moisture on low temperature mercury adsorption." *Carbon*, 40, 65–72.

Li, Y. H., Lee, C. W., and Gullett, B. K. (2003). "Importance of activated carbon's oxygen surface functional groups on elemental mercury adsorption." *Fuel*, 82, 451–457.

Manocha, S. M. (2003). "Porous carbons." *Sadhana*, 28, 335–348.

Martin, R. J., and Ng, W. J. (1987). "The repeated exhaustion and chemical regeneration of activated carbon." *Water Res.*, 21(8), 961–965.

Matatov-Meytal, Y. I., and Sheintuch, M. (1997). "Abatement of pollutants by adsorption and oxidative catalytic regeneration." *Ind. Eng. Chem. Res.*, 36(10), 4374–4380.

Matatov-Meytal, Y. I., Sheintuchi, M., Shter, G. E., and Grader, G. S. (1997). "Optimal temperatures for catalytic regeneration of activated carbon." *Carbon*, 35(10–11), 1527–1531.

Mundale, V. D., Joglekar, H. S., Kalam, A., and Joshi, J. B. (1991). "Regeneration of spent activated carbon by wet air oxidation." *Can. J. Chem. Eng.*, 69, 1149–1159.

Pope, J. P. (1996). *Activated carbon and some applications for the remediation of soil and groundwater pollution*.

San Miguel, G., Lambert, S. D., and Graham, N. J. D. (2001). "The regeneration of field spent granular activated carbons." *Water Res.*, 35(11), 2740–2748.

Sheintuch, M., and Matatov-Meytal, Y. I. (1999). "Comparison of catalytic processes with other regeneration methods of activated carbon." *Catal. Today*, 53, 73–80.

Sing, K. S. W., Everett, D. H., Haul, R. A. W., Moscou, L., Pierotti, R. A., Rouquerol, J., and Siemieniewska, T. (1985). "Reporting physisorption data for gas/solid systems: With special reference to the determination of surface area and porosity." *Pure Appl. Chem.*, 57(4), 603–619.

Skodras, G., Diamantopoulou, Ir., Natas, P., Palladas, A., and Sakellaropoulos, G. P. (2005). "Postcombustion measures for cleaner solid fuels combustion: Activated carbons for toxic pollutants removal from flue gases." *Energy Fuels*, 19(6), 2317–2327.

Van Vliet, B. M. (1991). "The regeneration of activated carbon." *J. S. Afr. Inst. Min. Metall.*, 91(5), 159–167.

Walker, P. L., Jr., Taylor, R. L., and Ranish, J. M. (1991). "An update on the carbon-oxygen reaction." *Carbon*, 29(3), 411–421.